SOLAR LIMB DARKENING

I: λλ(3033–7297)

A. KEITH PIERCE and CHARLES D. SLAUGHTER
Kitt Peak National Observatory, Tucson, Arizona*

(Received 29 June, 1976)

Abstract. The coefficients of several polynomial representations of the limb darkening at 62 wavelengths in the UV and visible portions of the solar spectrum obtained at the McMath Solar Telescope are presented in tabular form. Full corrections for scattered light and seeing have been included in the reductions.

> "It is important to draw attention to the simplicity of the theory of the darkening of the Sun's disc towards the limb. It is a consequence simply and solely of the temperature gradient in the outer layers."
> E. A. Milne (1930)

1. Introduction

The importance of 'the limb' has long been recognized in observational work at the McMath Solar Telescope. Indeed, the telescope was built with a large image scale, in part, to permit work at the extreme limb. This work capitalizes on that ability and the availability of sensitive detectors with short time constant circuitry, a high resolution double pass spectrometer free of scattered light and modern computers which make it feasible to acquire and handle a large volume of data.

2. The Observing Program

The continuum solar spectrum is well defined in the red and infrared. In contrast, in the region below 5000Å the saturation of Fraunhofer lines leaves few if any windows. Furthermore, since the absolute intensities in these windows are poorly known, the quality of the window is unknown. In order to be somewhat independent of the absolute quality, a large number of windows were selected from the preliminary Kitt Peak solar atlas. The selection was based on the width of the window, since solar rotation slightly shifts the wavelength of observation, and upon the appearance of a local continuum in the atlas. Eight of Houtgast's (1970) list of 32 ultraviolet high points have been included.

Observations were obtained on 14 days in the period March, 1974 through January, 1975 at the 77-cm primary image of the McMath Solar Telescope at Kitt Peak. An observation consisted of digitally sampling the spectrometer output as the image drifted by diurnal motion across the entrance aperture. This method was selected in the belief that there is no difference between polar and equatorial darkening since the

* Operated by the Association of Universities for Research in Astronomy, Inc., under contract with the National Science Foundation.

Solar Physics **51** (1977) 25–41.

recent work by Altrock and Canfield (1972), Caccin *et al.* (1970) and Falciani *et al.* (1974) has demonstrated that there are no detectable variations in temperature between pole and equator. Any scans which were perturbed because of the presence of sunspots or facular regions have been rejected.

The spectrometer was used in double pass to permit determination of the internal scattered light and with a prism predisperser to eliminate overlapping orders. The 10 mm × 0.1 mm entrance slit was oriented perpendicular to the E–W drift and centered with respect to the solar image. By stopping the telescope drive a four-minute drift curve, two minutes on and two off the Sun, made up an observation of 4096 data elements. The detector output from the S20 photomultiplier was fed through a preamplifier to a low-pass, band-limited (400 Hz cut-off frequency) amplifier and digitized at 1 kHz. Sixty-three consecutive digitizations were summed by an on-line computer and each sum was recorded on magnetic tape. To permit determination of the scattered light and to measure amplifier offsets, the spectrometer intermediate shutter was closed for four brief intervals during a scan. These 'closures' were taken near the disk center, and also near $R = 1.2$ and $R = 1.9$.

3. Data Reduction

The observed drift curves do not represent the true limb darkening because of limitations in the recording system, stray light from sky and telescope and seeing. It is the purpose of this section to discuss methods of restoration which yield the best values of the limb darkening.

An example of a typical drift curve is shown in Figure 1. The curves are characterized by an abrupt limb discontinuity and by a central region where fluctuations are due primarily to the solar granulation field. It is possible to reduce the granulation and photocell noise by filtering, through application of Fourier transform techniques; however, if the sharp limb profile is to be maintained, as it must, the Fourier transform method will not help reduce the fluctuations at the center of the disc. Lites (1972) considered this problem and developed a technique which he called "filtering in the small", by which the effective width of the filter is adjusted according to the local curvature of the filtered function. However, here it was felt that it was better to carry the raw data through the restoration process with a minimum of smoothing.

Since the final results were to be reported in the $I(\mu = \cos\theta)$ plane all of the approximately 2000 data points were transformed from the observed $I(\sin\theta)$ plane to the $I(\mu)$ plane and then normal points were formed. This had the effect of smoothing the data as well as reducing the number of data elements in an observation. For example, the normal point nearest the disc center at $\mu \simeq 0.975$ includes all points from $\mu = 1.0$ to 0.95 or from $\sin\theta = 0.0$ to 0.312; for the normal point at $\mu \simeq 0.175$ in the interval $\mu = 0.20$ to 0.15 the sin ranges from 0.9798 to 0.9887, etc. With this subdivision the normal point at $\mu \simeq 0.975$ contains about 318 observation points whereas the point at $\mu \simeq 0.175$ contains only 9 points. This will be considered further in the discussion of the least square fit to the observations.

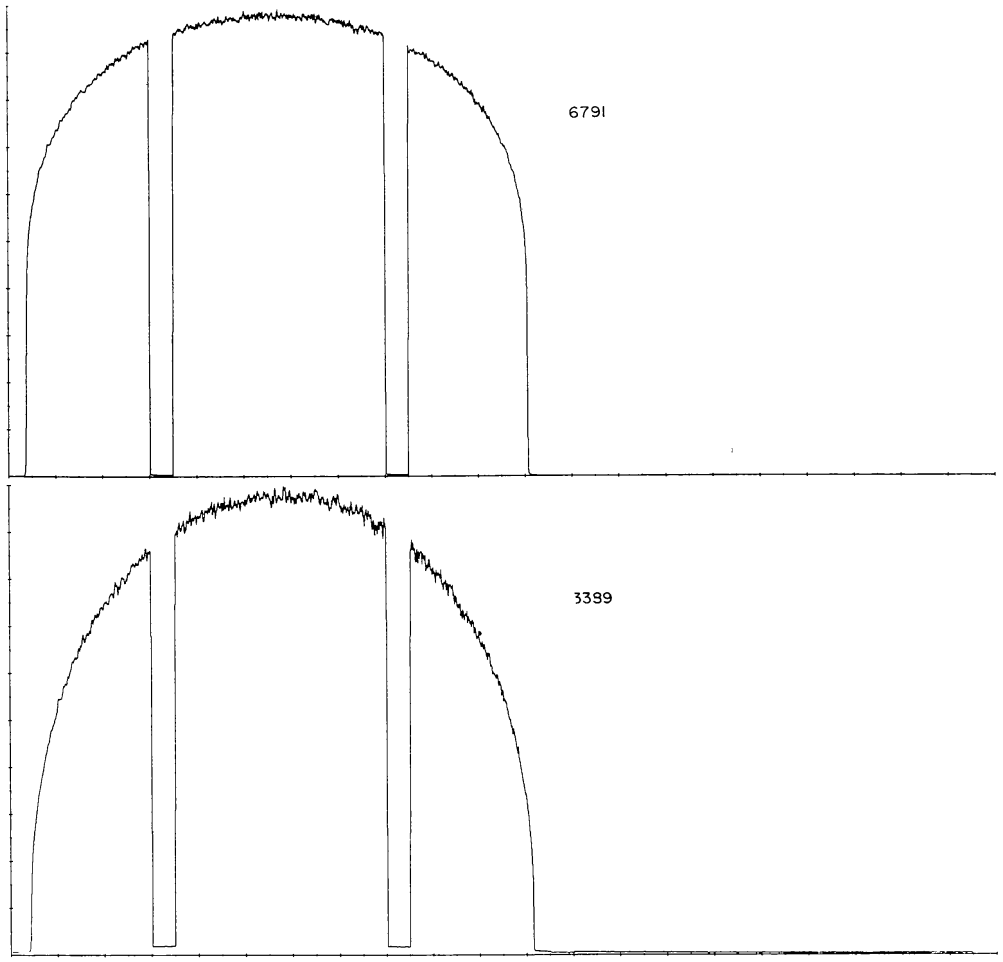

Fig. 1. Drift curve taken at λ6791 Å and λ3389 A.

Several factors contribute to the spread function (Raudenbusch, 1938); these are blurring caused by: (a) seeing, (b) atmospheric and telescopic scattered light, (c) slit width and height, and (d) time constant or lag in the drift curves. In this case explicit correction for slit width is not necessary since the width employed was $\frac{1}{4}$ s of arc and its spread function may be included in the seeing function. The maximum error due to a slit length of 1 cm together with a 77-cm image is a few thousandths of a percent and thus can be neglected. The time constant of the recording system was $\frac{1}{400}$ s which corresponds in a drift curve to an integration over $\frac{1}{25}$ s of arc and also has a negligible influence; seeing and scattered light remain.

3.1. Zero correction

As shown in Figure 1 the drift curve has several zeros obtained by closing the intermediate shutter of the spectrograph. The zero, obtained while scanning the Sun's image, represents the scattered light in the spectrograph system. Since the intensity in this zero, call it $I(z)$, is proportional to the light I entering the spectrograph, each point of the drift curve has a zero value of $I(z) \cdot I$ which was subtracted from the observed curve to give the corrected observed limb darkening.

3.2. Determination of the position of the limbs

Three techniques for determining the limb point were tried: (1) from the known angular diameter of the Sun the time-length of the drift curve could be calculated and compared with the observed, (2) location of the limb by selecting points at the beginning and end of the drift curves having one half of the extrapolated limb intensity, and (3) determination of the inflection points of the limb by numerical differentiation. Method (3) appeared to be best and was used in nearly all of our reductions. Method (1) assumes a knowledge of the solar diameter. Wittmann's (1973) value does not agree with our observations which seem to require a smaller angular solar diameter. Method (2) works well but like method (3) depends on the smoothness of the limb profile – stability of the seeing and freedom of image motion. For a simple step function atmospheric blurring does not change the position of the limb inflection point. However in the limb darkened case the diameter is augmented. Hill *et al* (1975) discuss this in their paper on the definition of an edge on the solar disc; their finite Fourier transform definition is not applicable here.

3.3. Correction for scattered light and blurring

Since various authors differ in their terminology we define here the terms that are used. By stray light is meant light lost from an elemental area of the object in transversing the Earth's atmosphere and the optical system and appearing elsewhere in the corresponding image of the object. Scattered light is that portion scattered at angles from 0° to 90° by aerosols, dust in the atmosphere and by diffraction as well as by dirty, scratched and generally imperfect optics. Blurring, commonly called seeing, refers to displacements caused by refractive index inhomogeneities in the Earth's atmosphere and is generally limited to small angles – 0 to 10″.

The estimation of the magnitude and the correction for stray light has been considered by many workers; a few of the references are: Wanders (1934), David and Elste (1962), Zwann (1965), Staveland (1970, 1972), and Mullan (1973). After consideration of various approaches to the problem, we felt that the most satisfactory treatment was that of Brahde (1972, 1974) who used a method of numerical integration. The authors are very grateful to him for supplying his program and for his advice in its use. The observed intensity at point P (Figure 2) is obtained by integrating the stray light $\psi(\rho)$ from every point on the disc:

$$S(x_0 y_0) = \int_{\phi_1}^{\phi_2} \int_{\rho_1}^{\rho_2} f(R^2)\psi(\rho)\rho \, \mathrm{d}\rho \, \mathrm{d}\phi, \tag{1}$$

where $f(R^2)$ is the intensity i.e., the true limb darkening at Q. It is interpolated from a table of limb darkening given in λ and $\cos\theta$; R^2 instead of R is used to avoid a square root in the computation; $\psi(\rho)$ is the stray light function

$$\psi(\rho) = \psi_b(\rho) + \psi_s(\rho) = (1-\varepsilon)\left[\frac{1-m}{\pi b_1^2} e^{-(\rho/b_1)^2} + \frac{m}{\pi b_2^2} e^{-(\rho/b_2)^2}\right] + \frac{\varepsilon A}{B^{2q} + \rho^{2q}}, \tag{2}$$

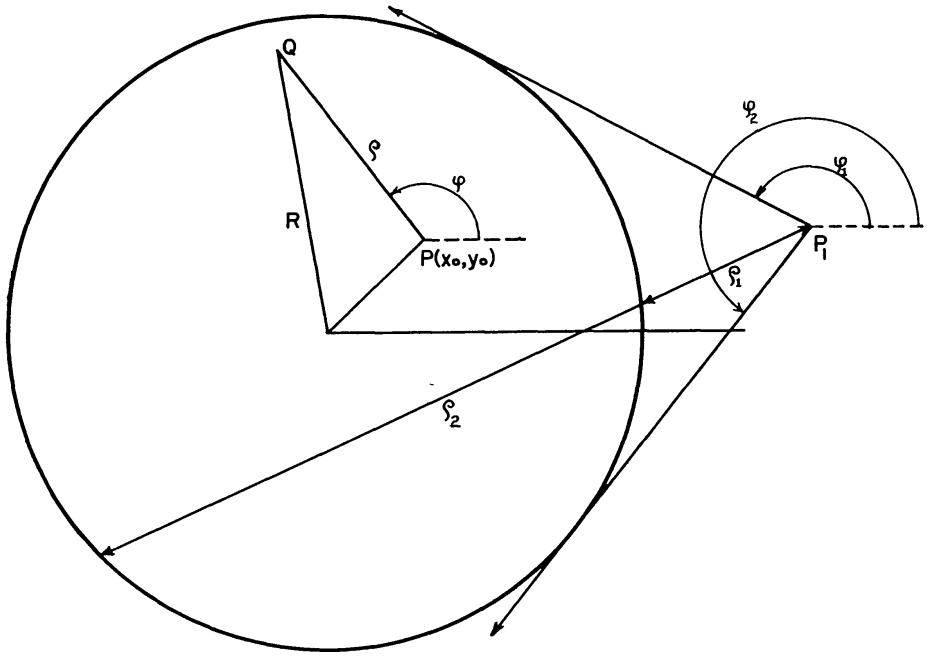

Fig. 2. The geometry of the scattering.

where A is a normalizing factor, ε and B are scattering parameters and b_1, b_2 and m are the blurring parameters. The quantity q is the new parameter introduced by Brahde. The integration in ρ is performed by combination of a 9 point Gaussian integration and a Romberg integration with an accuracy of 5×10^{-4} in intensity. In previous work, aureoles were best fit by $q = 1.0$ and by B approaching zero. However as shown by David and Elste (1962) this introduces a logarithmic singularity at the center of the disc and is one of the reasons others have tried to represent the scattering by sums of exponentials. Brahde avoids this difficulty by assigning a fixed value of B and allows q to be a new parameter (another part of his program also allows B to be a free parameter). A value of 0.3 was assumed for B with the radius $R = 16'$ ($R = 1.0$). For each observation, from 14 points off the disc in the interval $R = 1.046$ to $R = 1.400$, 12 points in the region of the limb $R = 1.0015$ to $R = 0.9985$ and 10 points on the disc Equation (1) is iteratively solved for the parameters ε, m, b_1, b_2, and q of the stray light function and their errors by making a fit to the observed profile of the limb darkening, blurring and scattered light. Figure 3(A) gives statistics for the descending limb and reveals that the mean seeing profile has a full width at half intensity $2b_1\sqrt{\ln 2}$, of 2.9″. The corresponding mean $\bar{b}_2 = 8''.1$ with $\bar{m} = 0.096$.

Because runs at different wavelengths were made on different dates it is not possible to summarize the scattering parameters in a very meaningful way, however averages and trends to appear which allow the reader to form an opinion of the results. In Figure 3(B) q is plotted as a function of λ. In Figure 3(C) we see that with clean mirrors the intensity at λ3400 at a distance of 44 arc sec off the limb ($R = 1.046$) amounted to 0.1%; with dirty mirrors and poor sky conditions the value rose to 0.6%. At this point the reader should be reminded that the observations were made with the

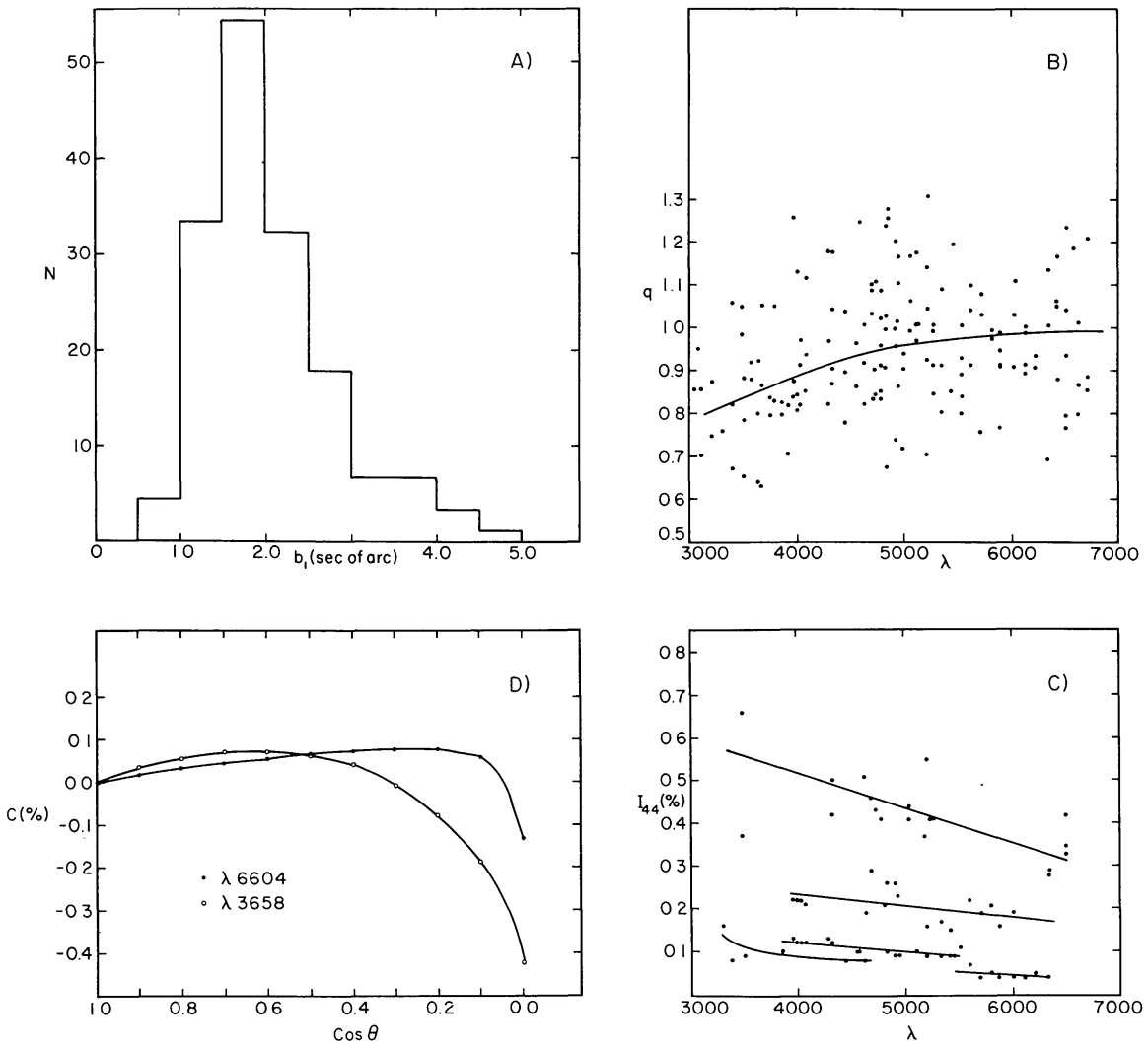

Fig. 3. (A) Distribution of the Gaussian blurring parameter b_1, Equation (2). (B) Values of the exponential factor q of Equation (2). (C) The observed intensity 44″ from the limb for a few selected observing periods. (D) The mean difference between the true and observed limb darkening for two wavelengths as a function of cos θ.

McMath Solar Telescope, a vignetted instrument in the sense that the illumination of the concave image forming mirror by sunlight from the heliostat falls to zero at about one solar diameter from the limb. This considerably alters the scattering. Hence, we expect the true scattering function to be more complex than Equation (2) but note that this vignetting condition is not obtained in the range used for the solution of q and ε, however, it does make the meaning of A ambiguous. David and Elste suggested ratioing $S(R)$ obtained from the calculation with the observed scattering, off the limb, and solving for the normalizing factor εA as follows. Let ε by the small fraction of the radiation that is scattered, $I(R)$ and $I'(R)$ be the true and observed intensities, then

$$I'(R)=(1-\varepsilon)I(R)+\varepsilon I(0)AS(R). \tag{3}$$

When compared with the center of the disc,

$$\frac{I(R)}{I(0)}=\frac{\dfrac{I'(R)}{I'(0)}-\dfrac{A\varepsilon I(0)}{I'(0)}S(R)}{1-\dfrac{A\varepsilon I(0)}{I'(0)}S(0)}. \tag{4}$$

The factor $AI(0)/I'(0)$ can be determined from any of the 14 points outside the limb where the true intensity in zero; here

$$\frac{I'(R)}{I'(0)}\approx\frac{A\varepsilon I(0)}{I'(0)}S(R) \tag{5}$$

and

$$\frac{A\varepsilon I(0)}{I'(0)}=\frac{1}{S(R)}\ \frac{I'(R)}{I'(0)}\equiv\frac{1}{14}\sum_{1}^{14}\frac{I'(R)/I'(0)}{S(R)}=K. \tag{6}$$

The difference between the true and observed limb darkening is

$$C\equiv\frac{I(R)}{I(0)}-\frac{I'(R)}{I'(0)}=\frac{KS(0)}{1-KS(0)}\left[\frac{I'(R)}{I'(0)}-\frac{S(R)}{S(0)}\right]. \tag{7}$$

Rather than determine the proportionality factor from a single off-limb point the average of 14 points was used. The correction to the observed limb darkening is satisfactorily small. Two of the correction curves from Equation (7) are illustrated by Figure 3(D).

The kernel of the blurring, i.e., b_1, essentially determines the observed slope at the limb. The correction of the solar limb profile for seeing has been treated by Wanders (1934) and Minnaert *et al.* (1949) and many others. This problem is the classical one of solving an integral equation for the true distribution perturbed with a known Gaussian error distribution; there are many many solutions and techniques for solution available.

Eddington's (1913) method was adopted, obtaining the second and fourth differences by numerical differentiation. As with most of the truncated methods there is a strong tendency for Gibbs' phenomena to appear because of the step nature of the limb. This oscillation has required some smoothing. Guidance is obtained by observing that an undarkened limb, that is a step function, smeared by a Gaussian results in a symmetrical S-shaped profile. The restoration is direct and can be accomplished by restoring light beyond the limb (the point of inflection) symmetrically to the points within the limb.

Figure 4 shows as an example the observed ascending limb at $\lambda=6791$ and the restoration. This is a particularly favorable case. For many observations seeing fluctuations cause greatly magnified derivative fluctuations and more judgment is required in the restoration. In a small percentage of the observations no restoration is possible—within the strict limits of quality that were imposed. In all of this series of observations the blurring corrections have only modified the points closer to the limb than $\cos\leqslant 0.1$, otherwise the observations have been rejected because of poor seeing.

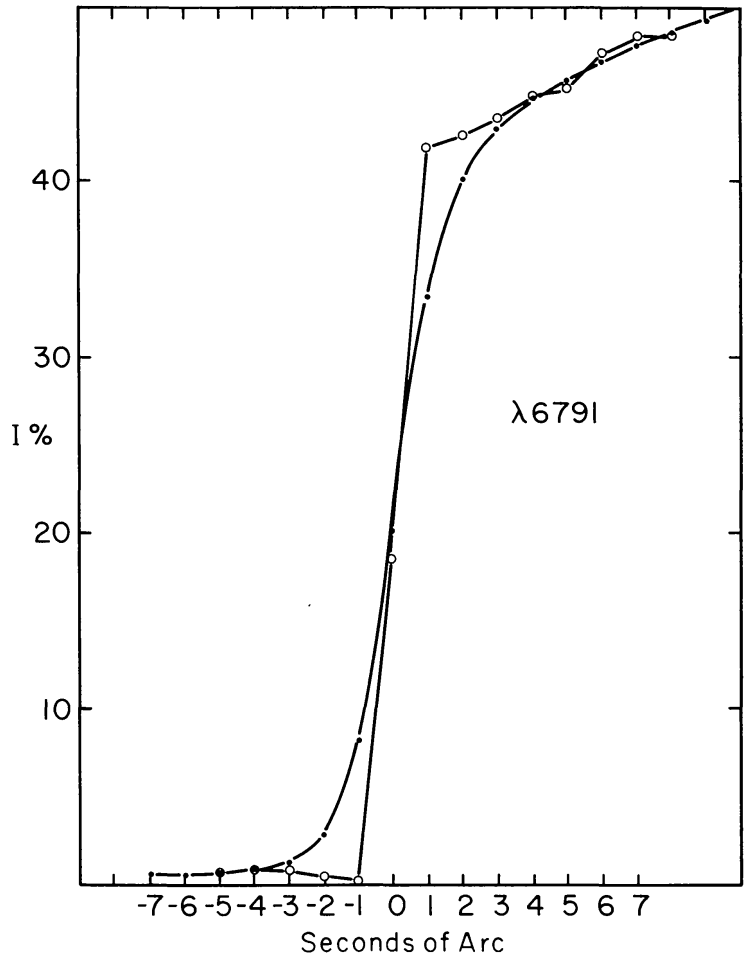

Fig. 4. Limb restoration with a Gaussian profile.

4. Least Square Fit to the Observations

After correcting the observations a least square fit was made to the 18 normal points together with a few extreme limb points taken from the days of best seeing. The question is how to weight the observations. The points near the center of the disc show fluctuations due to the granulation field. Near the limb they are smoothed by the projection factor (Figure 1). An examination of the $I(\cos\theta)$ plots and the deviations of the normal points from a smooth curve leads one to the conclusion that all normal points should be given approximately equal weight independent of the number of data points that were summed to form a normal point. We have arbitrarily used $n^{1/4}$ as the weight in the tables thus giving a weight of 4.2 to the $\cos\theta = 0.975$ point and a weight of 1.0 at the extreme limb. Equal weights for all points have also been tried. The difference between the two solutions is less than 0.2%.

Several power series have been tried. A good representation to the limb darkening is given by Sykes' (1953) formula:

$$I(\lambda, \xi) = a(2) + b(2)\xi + c(2)\xi^2, \tag{8}$$

where $\xi = 1n\ \mu$; $\cos\theta = \mu$. The coefficients for each λ are given in Table I. The second

TABLE I
Coefficients of 2nd degree, ln μ, fit to the limb darkening

λ	No.	$a(2)$	$b(2)$	$c(2)$
3033.27	4	1.00000	0.81773	0.21103
3069.82	6	1.00000	0.72281	0.14836
3108.43	6	1.00000	0.70827	0.14319
3204.68	8	1.00000	0.69896	0.14241
3298.97	8	1.00000	0.66442	0.13055
3389.53	8	1.00000	0.63905	0.12218
3499.49	8	1.00000	0.64091	0.12817
3563.52	10	1.00000	0.64312	0.12988
3626.50	6	1.00000	0.62074	0.12442
3658.75	6	1.00000	0.60464	0.11690
3740.88	10	1.00000	0.64219	0.12761
3779.92	5	1.00000	0.63963	0.12675
3852.02	8	1.00000	0.67421	0.14195
3909.28	8	1.00000	0.66030	0.13914
3954.25	8	1.00000	0.65565	0.14273
3988.15	8	1.00000	0.63352	0.13039
4019.70	10	1.00000	0.63598	0.13157
4069.44	8	1.00000	0.62932	0.12916
4117.23	3	1.00000	0.60339	0.11906
4163.20	4	1.00000	0.60556	0.11891
4219.05	4	1.00000	0.59521	0.11639
4279.30	6	1.00000	0.59150	0.11794
4316.45	6	1.00000	0.56951	0.10978
4438.85	6	1.00000	0.53473	0.08932
4451.25	2	1.00000	0.56391	0.10810
4543.55	4	1.00000	0.58047	0.12433
4567.92	6	1.00000	0.57630	0.12478
4573.45	4	1.00000	0.57741	0.12256
4615.10	6	1.00000	0.53486	0.09919
4683.06	6	1.00000	0.52465	0.09427
4719.00	8	1.00000	0.52148	0.09364
4774.35	12	1.00000	0.52923	0.10021
4811.57	6	1.00000	0.52083	0.09674
4830.75	8	1.00000	0.51171	0.09357
4905.60	8	1.00000	0.52134	0.10216
4929.05	8	1.00000	0.50385	0.09154
4980.90	6	1.00000	0.48759	0.08261
5038.00	7	1.00000	0.49370	0.08952
5102.10	8	1.00000	0.49195	0.08882
5199.30	10	1.00000	0.48407	0.08841
5256.35	8	1.00000	0.46384	0.07713
5334.60	6	1.00000	0.47846	0.08911
5417.60	4	1.00000	0.46016	0.07976
5522.00	8	1.00000	0.43974	0.07222
5599.50	6	1.00000	0.43682	0.07257
5695.60	6	1.00000	0.43447	0.07376
5798.80	6	1.00000	0.43087	0.07488
5874.30	12	1.00000	0.42491	0.07218
6010.15	8	1.00000	0.41608	0.06985
6109.75	14	1.00000	0.41338	0.07082

Table I (Continued)

λ	No.	$a(2)$	$b(2)$	$c(2)$
6205.90	8	1.00000	0.40442	0.06892
6326.00	6	1.00000	0.39070	0.06287
6409.70	6	1.00000	0.38515	0.06241
6492.50	8	1.00000	0.38448	0.06276
6604.00	8	1.00000	0.35975	0.05174
6694.00	10	1.00000	0.36955	0.05849
6791.40	8	1.00000	0.36693	0.05949
6916.00	7	1.00000	0.35500	0.05539
7008.75	7	1.00000	0.35316	0.05590
7104.25	6	1.00000	0.35605	0.05778
7199.25	9	1.00000	0.34884	0.05492
7296.75	6	1.00000	0.34290	0.05318

column gives the number of observations used in the mean, which equals the number of $\frac{1}{2}$ drift curves. The following three columns give $a(2)=1.0$ and the values of $b(2)$ and $c(2)$ from a least square solution. The residuals when plotted show a systematic trend with $\cos\theta$ as illustrated in Figure 5 suggesting that a higher degree polynomial would have given a better fit. Accordingly a 5th order least squares fit of the observations to the series

$$I(\lambda,\xi)=a(5)+b(5)\xi+c(5)\xi^2+d(5)\xi^3+e(5)\xi^4+f(5)\xi^5 \tag{9}$$

was performed giving the coefficients in Table II. The probable error of a single normal point as obtained from the scatter about Equation (9) is listed in the last column.

Since the representation

$$I(\lambda,\mu)=A(2)+B(2)\mu+C(2)\mu^2 \tag{10}$$

often appears in the literature we list in Table III its coefficients from a least square solution. Table IV gives the coefficients of a 5th order fit to the observations from the equation

$$I(\lambda,\mu)=A(5)+B(5)\mu+C(5)\mu^2+D(5)\mu^3+E(5)\mu^4+F(5)\mu^5 \tag{11}$$

and the probable error of a single normal point.

The residuals, observed minus computed, from the second degree Equation (10), as illustrated by Figure 6 are systematic in μ and a function of wavelength. However at $\lambda\approx4000$ Å the $\cos^2\theta$ representation is a good fit to the observations and the residual curve is nearly a straight line with deviations less than 0.3%.

The fifth degree polynomials represent our observations very well. They can be considered very reliable to $\cos\theta=0.1$ and they may be projected to $\cos\theta=0.05$ with some confidence.

The extension of this work to λ24018 is given in Paper II.

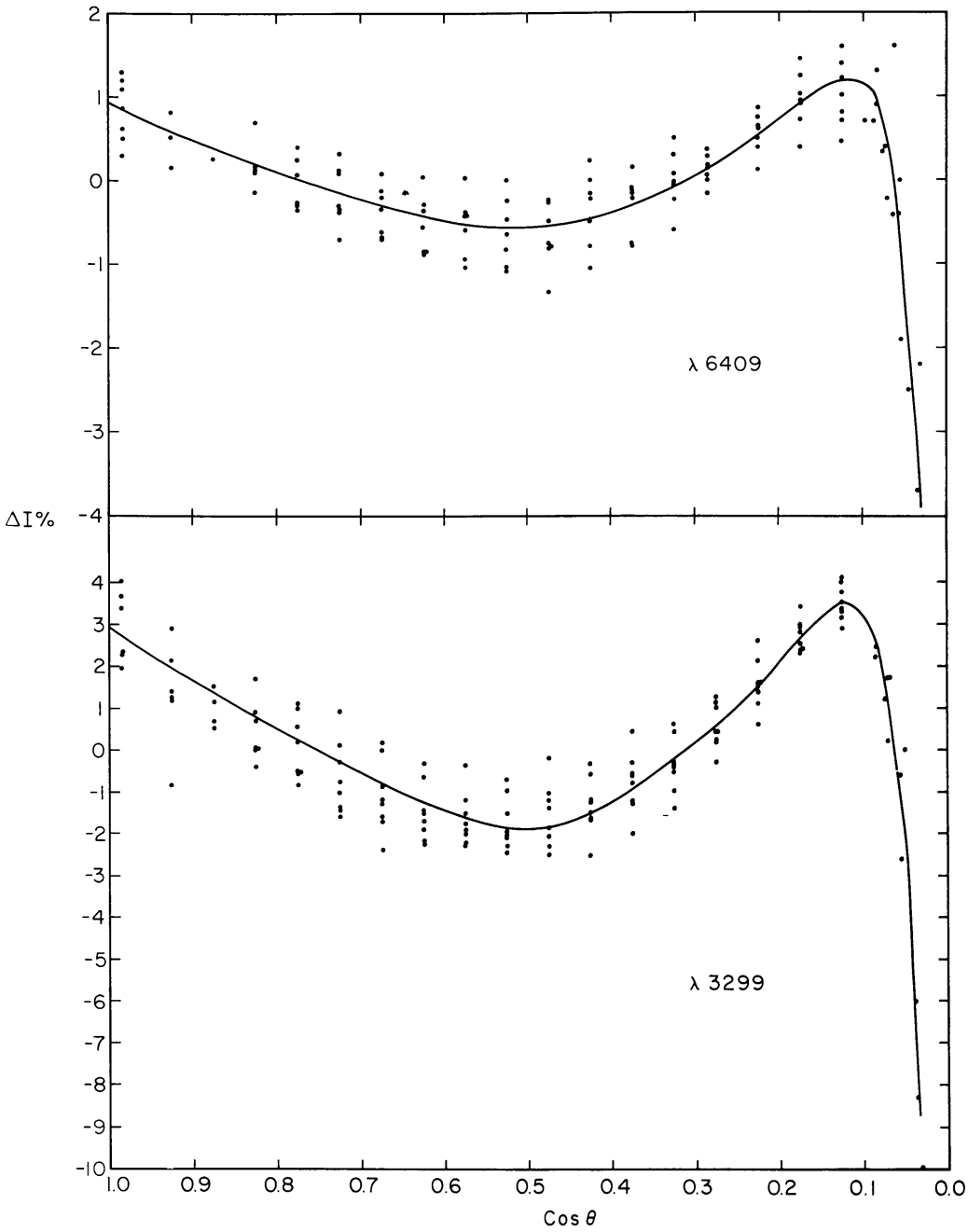

Fig. 5. Residuals, observed minus computed, for the normal points and Equation (8).

TABLE II

Coefficients of 5th degree, ln μ, fit to the limb darkening, Equation (9)

λ	No.	$a(5)$	$b(5)$	$c(5)$	$d(5)$	$e(5)$	$f(5)$	$Pe \times 10^4$
3033.27	4	1.00000	0.97019	0.52334	0.23153	0.08514	0.01478	79
3069.82	6	1.00000	0.90116	0.35235	0.04708	−0.00600	−0.00164	86
3108.43	6	1.00000	0.90333	0.40472	0.11113	0.02068	0.00195	58
3204.68	8	1.00000	0.87103	0.37246	0.09625	0.01712	0.00157	49
3298.97	8	1.00000	0.81884	0.33404	0.08388	0.01473	0.00135	47
3389.53	8	1.00000	0.77698	0.29530	0.06644	0.01050	0.00090	47
3499.49	8	1.00000	0.75452	0.27592	0.05559	0.00742	0.00061	44
3563.52	10	1.00000	0.74606	0.26455	0.04958	0.00578	0.00044	42
3626.50	6	1.00000	0.72148	0.27406	0.07379	0.01675	0.00198	31
3658.75	6	1.00000	0.68443	0.21916	0.03790	0.00512	0.00048	39
3740.88	10	1.00000	0.72647	0.19643	−0.01482	−0.01775	−0.00255	51
3779.92	5	1.00000	0.72880	0.21602	0.00547	−0.01131	−0.00200	48
3852.02	8	1.00000	0.79182	0.27120	0.01898	−0.01041	−0.00187	66
3909.28	8	1.00000	0.80076	0.33477	0.08431	0.01479	0.00143	37
3954.25	8	1.00000	0.78644	0.31546	0.05927	0.00309	−0.00028	40
3988.15	8	1.00000	0.74422	0.28048	0.05993	0.00881	0.00081	40
4019.70	10	1.00000	0.75222	0.29228	0.06451	0.00821	0.00041	48
4069.44	8	1.00000	0.74615	0.30280	0.08672	0.02051	0.00258	38
4117.23	3	1.00000	0.68191	0.20760	0.01721	−0.00476	−0.00096	52
4163.20	4	1.00000	0.69661	0.22354	0.02358	−0.00398	−0.00098	37
4219.05	4	1.00000	0.70411	0.24501	0.03626	−0.00003	−0.00036	46
4279.30	6	1.00000	0.68623	0.25109	0.05684	0.00879	0.00061	35
4316.45	6	1.00000	0.63476	0.18128	0.01269	−0.00384	−0.00060	51
4438.85	6	1.00000	0.63187	0.15325	−0.03962	−0.03059	−0.00431	58
4451.25	2	1.00000	0.65346	0.23609	0.05891	0.01119	0.00098	39
4543.55	4	1.00000	0.64906	0.25609	0.09393	0.03437	0.00620	22
4567.92	6	1.00000	0.63505	0.23800	0.08422	0.03396	0.00669	25
4573.45	4	1.00000	0.63825	0.21697	0.03502	−0.00240	−0.00167	29
4615.10	6	1.00000	0.63059	0.23363	0.06686	0.01644	0.00194	38
4683.06	6	1.00000	0.61905	0.21131	0.04269	0.00543	0.00031	41
4719.00	8	1.00000	0.60534	0.19201	0.02948	0.00098	−0.00023	43
4774.35	12	1.00000	0.60109	0.18965	0.02545	−0.00152	−0.00065	35
4811.57	6	1.00000	0.60697	0.22382	0.06146	0.01239	0.00113	27
4830.75	8	1.00000	0.56822	0.13860	−0.01766	−0.01860	−0.00305	40
4905.60	8	1.00000	0.59364	0.22652	0.07044	0.01543	0.00124	40
4929.05	8	1.00000	0.57937	0.17967	0.01777	−0.00664	−0.00171	37
4980.90	6	1.00000	0.57954	0.19439	0.03580	0.00178	−0.00023	48
5038.00	7	1.00000	0.58593	0.22227	0.06485	0.01411	0.00141	32
5102.10	8	1.00000	0.55333	0.15371	0.00587	−0.00864	−0.00176	41
5199.30	10	1.00000	0.54874	0.16891	0.02309	−0.00185	−0.00084	35
5256.35	8	1.00000	0.55558	0.19726	0.05154	0.00975	0.00094	55
5334.60	6	1.00000	0.54586	0.19578	0.05881	0.01464	0.00164	38
5417.60	4	1.00000	0.52297	0.15019	0.00871	−0.00937	−0.00214	35
5522.00	8	1.00000	0.52371	0.18426	0.05607	0.01457	0.00175	41
5599.50	6	1.00000	0.52256	0.18875	0.05678	0.01368	0.00154	38
5695.60	6	1.00000	0.50895	0.18154	0.05814	0.01563	0.00190	36
5798.80	6	1.00000	0.50411	0.18599	0.06394	0.01821	0.00225	28
5874.30	12	1.00000	0.48373	0.14326	0.02268	0.00114	0.00010	36
6010.15	8	1.00000	0.48546	0.16981	0.05093	0.01203	0.00128	48
6109.75	14	1.00000	0.47558	0.16759	0.05449	0.01455	0.00176	31
6205.90	8	1.00000	0.45476	0.13115	0.02442	0.00451	0.00057	39

Table II (Continued)

λ	No.	a(5)	b(5)	c(5)	d(5)	e(5)	f(5)	$Pe \times 10^4$
6326.00	6	1.00000	0.44719	0.12509	0.01779	0.00070	−0.00009	35
6409.70	6	1.00000	0.42944	0.10246	−0.00037	−0.00640	−0.00109	27
6492.50	8	1.00000	0.41974	0.09330	−0.00265	−0.00591	−0.00087	34
6604.00	8	1.00000	0.42448	0.14233	0.05239	0.01667	0.00232	51
6694.00	10	1.00000	0.40588	0.07744	−0.02111	−0.01471	−0.00222	33
6791.40	8	1.00000	0.41708	0.12512	0.02825	0.00528	0.00051	32
6916.00	7	1.00000	0.40433	0.12449	0.04060	0.01375	0.00210	32
7008.75	7	1.00000	0.37605	0.04890	−0.04052	−0.02141	−0.00310	52
7104.25	6	1.00000	0.38278	0.06829	−0.02772	−0.01989	−0.00343	22
7199.25	9	1.00000	0.38878	0.10099	0.01050	−0.00245	−0.00069	26
7296.75	6	1.00000	0.38376	0.09543	0.00163	−0.00751	−0.00153	39

TABLE III

Coefficients of 2nd degree, $\mu = \cos\theta$, fit to the limb darkening

λ	No.	A(2)	B(2)	C(2)
3033.27	4	0.06081	0.88702	0.05217
3069.82	6	0.05585	0.93310	0.01105
3108.43	6	0.06485	0.93547	−0.00032
3204.68	8	0.07316	0.95786	−0.03102
3298.97	8	0.08783	1.00460	−0.09243
3389.53	8	0.10214	1.01846	−0.12060
3499.49	8	0.11509	1.02225	−0.13734
3563.52	10	0.10992	1.04794	−0.15786
3626.50	6	0.13343	1.04097	−0.17440
3658.75	6	0.13263	1.07709	−0.20972
3740.88	10	0.11032	1.03152	−0.14184
3779.92	5	0.11488	1.02467	−0.13955
3852.02	8	0.11165	0.95102	−0.06267
3909.28	8	0.12834	0.93465	−0.06299
3954.25	8	0.15087	0.89224	−0.04311
3988.15	8	0.13840	0.98327	−0.12167
4019.70	10	0.13709	0.98538	−0.12247
4069.44	8	0.13860	0.99664	−0.13524
4117.23	3	0.14809	1.03250	−0.18059
4163.20	4	0.14649	1.01671	−0.16320
4219.05	4	0.16052	0.98575	−0.14627
4279.30	6	0.16877	1.00847	−0.17724
4316.45	6	0.17556	1.04454	−0.22010
4438.85	6	0.18829	1.00675	−0.19504
4451.25	2	0.18386	1.02456	−0.20842
4543.55	4	0.19993	1.00270	−0.20263
4567.92	6	0.21114	0.98303	−0.19417
4573.45	4	0.19976	1.00757	−0.20733
4615.10	6	0.21424	0.98662	−0.20086
4683.06	6	0.21495	0.99746	−0.21241
4719.00	8	0.21391	1.02090	−0.23481
4774.35	12	0.22045	1.01334	−0.23379
4811.57	6	0.22291	1.02487	−0.24778

Table III (Continued)

λ	No.	A(2)	B(2)	C(2)
4830.75	8	0.22889	1.02635	−0.25524
4905.60	8	0.24118	0.99745	−0.23863
4929.05	8	0.23872	1.01145	−0.25017
4980.90	6	0.22996	1.05565	−0.28561
5038.00	7	0.25576	0.97318	−0.22894
5102.10	8	0.25224	1.00468	−0.25692
5199.30	10	0.26958	1.97674	−0.24632
5256.35	8	0.25949	1.02402	−0.28351
5334.60	6	0.28320	0.96326	−0.24646
5417.60	4	0.27825	1.01520	−0.29345
5522.00	8	0.29462	0.98032	−0.27494
5599.50	6	0.30289	0.96670	−0.26959
5695.60	6	0.31378	0.95446	−0.26824
5798.80	6	0.32839	0.92579	−0.25418
5874.30	12	0.32602	0.95428	−0.28030
6010.15	8	0.33890	0.92949	−0.26839
6109.75	14	0.34653	0.92982	−0.27635
6205.90	8	0.36019	0.90010	−0.26029
6326.00	6	0.36131	0.91682	−0.27813
6409.70	6	0.37001	0.91338	−0.28339
6492.50	8	0.37276	0.91765	−0.29041
6604.00	8	0.36701	0.98044	−0.34745
6694.00	10	0.38256	0.92577	−0.30833
6791.40	8	0.39802	0.88437	−0.28239
6916.00	7	0.40344	0.89654	−0.29998
7008.75	7	0.40990	0.88664	−0.29654
7104.25	6	0.41575	0.87104	−0.28679
7199.25	9	0.41793	0.87530	−0.29323
7296.75	6	0.42318	0.87317	−0.29635

TABLE IV

Coefficients of 5th degree, $\mu = \cos\theta$ fit to the limb darkening, Equation (11)

λ	No.	A(5)	B(5)	C(5)	D(5)	E(5)	F(5)	$Pe \times 10^4$
3033.27	4	0.08209	0.79588	−0.32728	2.06684	−2.86649	1.24896	86
3069.82	6	0.05676	1.06900	−1.30706	3.85651	−4.45420	1.77899	77
3108.43	6	0.09543	0.55876	1.49102	−2.58685	2.10674	−0.66510	44
3204.68	8	0.11285	0.43717	2.14487	−3.95899	3.34427	−1.08018	30
3298.97	8	0.10747	0.74429	0.94300	−1.73573	1.30246	−0.36150	31
3389.53	8	0.12410	0.67282	1.52113	−3.30084	2.98399	−1.00119	22
3499.49	8	0.12823	0.82632	0.79318	−1.89980	1.75482	−0.60275	37
3563.52	10	0.11826	0.91395	0.49037	−1.32142	1.19064	−0.39180	46
3626.50	6	0.13936	0.90842	0.57929	−1.69932	1.63267	−0.56042	25
3658.75	6	0.14916	0.77226	1.45919	−3.76655	3.73016	−1.34421	25
3740.88	10	0.12416	0.88431	0.31220	−0.52936	0.22629	−0.01759	42

Table IV (Continued)

λ	No.	A(5)	B(5)	C(5)	D(5)	E(5)	F(5)	Pe × 10⁴
3779.92	5	0.14909	0.49352	2.39225	−5.16023	4.79409	−1.66872	48
3852.02	8	0.12050	0.89411	−0.08513	0.51261	−0.78562	0.34351	46
3909.28	8	0.14722	0.70713	0.78675	−1.34654	0.96062	−0.25519	24
3954.25	8	0.15460	0.88309	−0.17742	0.55979	−0.72001	0.29996	26
3988.15	8	0.14467	0.89214	0.25563	−0.64468	0.46452	−0.11229	29
4019.70	10	0.14955	0.79357	0.80727	−1.92346	1.78203	−0.60896	38
4069.44	8	0.13921	0.95294	0.21435	−0.94877	1.04342	−0.40114	22
4117.23	3	0.15291	0.92722	0.40800	−1.31498	1.25656	−0.42972	36
4163.20	4	0.14924	0.92492	0.39257	−1.28028	1.22131	−0.40776	21
4219.05	4	0.14229	1.20897	−0.98527	1.32989	−0.95423	0.25836	35
4279.30	6	0.17817	0.81981	0.88864	−2.43566	2.40735	−0.85832	31
4316.45	6	0.16193	1.18327	−0.71232	0.79948	−0.66418	0.23182	48
4438.85	6	0.17361	1.10375	−0.26439	−0.42657	0.70228	−0.28867	25
4451.25	2	0.18949	0.84249	0.89216	−2.54538	2.44361	−0.82238	25
4543.55	4	0.17323	1.24473	−1.01658	1.28417	−1.03759	0.35205	22
4567.92	6	0.20241	1.03191	−0.24672	−0.10145	0.17318	−0.05933	25
4573.45	4	0.17337	1.24027	−0.96185	1.13937	−0.89232	0.30116	30
4615.10	6	0.21636	0.88781	0.41845	−1.43503	1.35988	−0.44746	34
4683.06	6	0.20728	0.98836	0.33575	−1.95518	2.39340	−0.96960	24
4719.00	8	0.19517	1.16628	−0.31208	−0.90045	1.63721	−0.78614	36
4774.35	12	0.18640	1.35506	−1.30753	1.36181	−0.71541	0.11967	34
4811.57	6	0.20334	1.16792	−0.39899	−0.52057	1.00423	−0.45593	29
4830.75	8	0.18075	1.55637	−2.17983	3.05218	−2.25786	0.64839	40
4905.60	8	0.21868	1.15187	−0.59473	0.32977	−0.21553	0.10994	43
4929.05	8	0.20720	1.31845	−1.19989	1.18685	−0.67251	0.15990	38
4980.90	6	0.15765	1.98369	−4.16112	7.11363	−6.16512	2.07128	46
5038.00	7	0.23546	1.13724	−0.42727	−0.56643	1.19616	−0.57516	26
5102.10	8	0.23542	1.11424	−0.22720	−0.95708	1.48731	−0.65269	41
5199.30	10	0.24371	1.18310	−0.65500	−0.01018	0.53882	−0.30045	37
5265.35	8	0.19606	1.80914	−3.49586	5.81545	−5.02246	1.69766	48
5334.60	6	0.26814	1.03956	−0.19097	−0.71724	0.98599	−0.38547	38
5417.60	4	0.22874	1.54025	−2.15443	2.84347	−2.07225	0.61421	44
5522.00	8	0.24092	1.61047	−2.79815	4.46819	−3.75831	1.23687	46
5599.50	6	0.26152	1.43765	−2.08435	3.06146	−2.50085	0.82457	36
5695.60	6	0.27683	1.32126	−1.44120	1.53202	−0.89746	0.20855	37
5798.80	6	0.30505	1.13123	−0.78604	0.40560	0.02297	−0.07880	32
5874.30	12	0.27386	1.54420	−2.49821	3.62682	−2.79334	0.84667	43
6010.15	8	0.28868	1.43685	−2.06512	2.83402	−2.18212	0.68768	46
6109.75	14	0.29397	1.46821	−2.20076	3.05295	−2.34756	0.73318	37
6205.90	8	0.32519	1.26432	−1.44591	1.55723	−0.87415	0.17333	38
6326.00	6	0.31582	1.43155	−2.12408	2.79306	−1.94533	0.52897	35
6409.70	6	0.32895	1.37742	−1.94686	2.52875	−1.80945	0.52119	28
6492.50	8	0.31760	1.55474	−2.73710	4.12665	−3.29720	1.03531	36
6604.00	8	0.28202	2.12303	−5.18360	8.77765	−7.37497	2.37588	71
6694.00	10	0.32795	1.59699	−2.86022	4.06176	−2.95517	0.82869	39
6791.40	8	0.35330	1.38969	−2.14843	2.95067	−2.20553	0.66030	34
6916.00	7	0.34341	1.64280	−3.38592	5.55415	−4.70192	1.54749	41
7008.75	7	0.35749	1.52000	−2.83587	4.41525	−3.62975	1.17288	54
7104.25	6	0.36418	1.39244	−1.92836	2.04059	−1.00434	0.13549	33
7199.25	9	0.36025	1.50458	−2.59537	3.67122	−2.79112	0.85043	33
7296.75	7	0.34597	1.74631	−3.63929	5.64981	−4.53486	1.43207	41

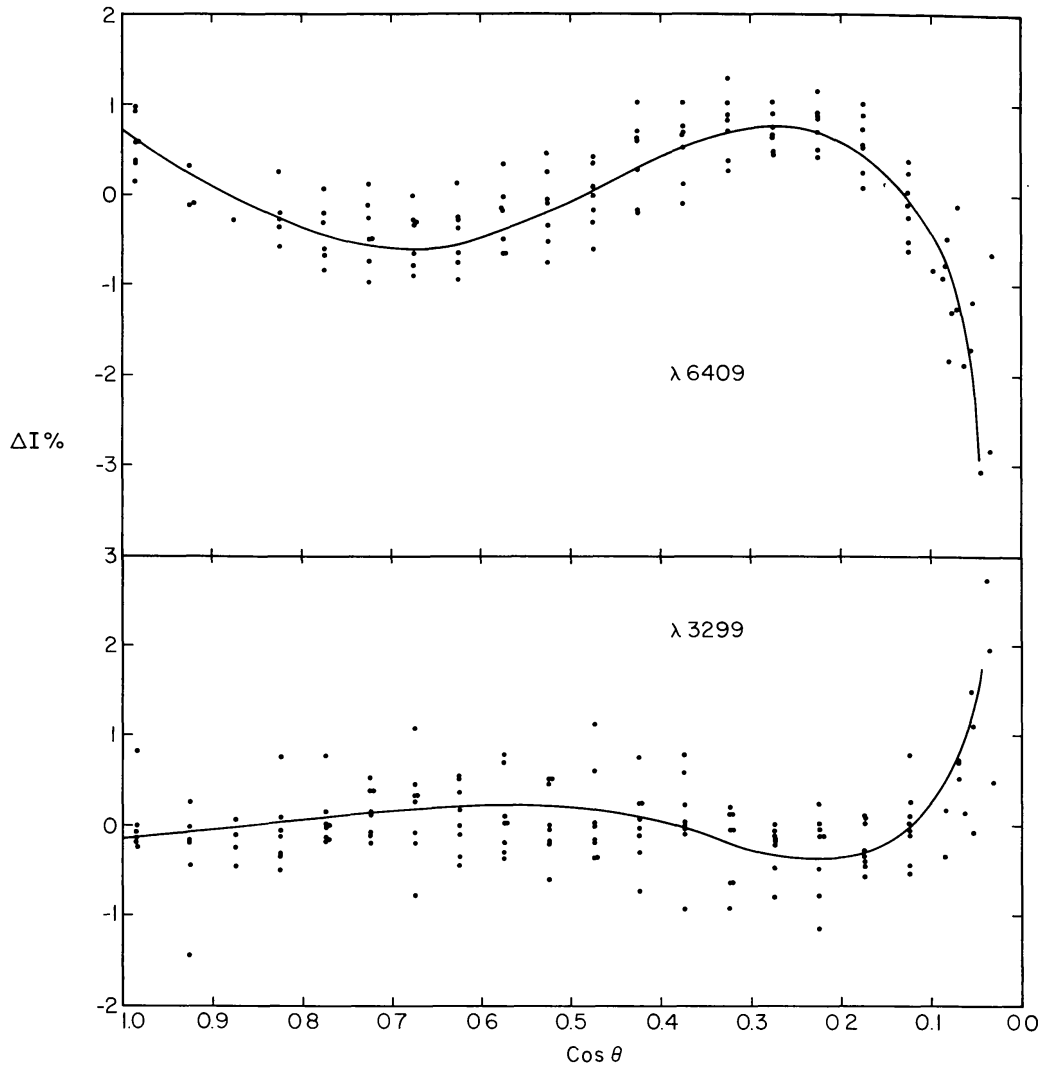

Fig. 6. Residuals, observed minus computed, for the normal points and Equation (10).

References

Altrock, R. C. and Canfield, R. C.: 1972, *Solar Phys.* **23**, 257.
Brahde, R.: 1972, *Solar Phys.* **26**, 318.
Brahde, R.: 1974, Inst. of Theor. Astrophys. Univ. Oslo, Report No. 41.
Caccin, B., Falciani, R., Moschi, G., and Rigutti, M.: 1970, *Solar Phys.* **13**, 33.
David, K. H. and Elste, G.: 1962, *Z. Astrophys.* **54**, 12.
Eddington, A. S.: 1913, *Monthly Notices Roy. Astron. Soc.* **73**, 359.
Falciani, R., Rigutti, M., and Roberti, G.: 1974, *Solar Phys.* **35**, 277.
Hill, H. A., Stebbins, R. T. and Oleson, J. R.: 1975, *Astrophys. J.* **200**, 484.
Houtgast, J.: 1970, *Solar Phys.* **15**, 273.
Lites, B. W.: 1972, N.C.A.R. Cooperative Thesis No. 28.
Milne, E. A.: 1930, *Handbuch der Astrophysik*, Vol. 3, Part 1, p. 145, Julius Springer, Berlin.
Minnaert, M., van den Hoven van Genderen, E. and van Diggelen, J.: 1949, *Bull. Astron. Inst. Neth.* **11**, 55.
Mullan, D. J.: 1973, *Solar Phys.* **32**, 65.
Raudenbusch, H.: 1938, *Astron. Nachr.* **266**, 301.

Staveland, L.: 1970, *Solar Phys.* **12**, 328.
Staveland, L.: 1972, Inst. Theor. Astrophys. Univ. Oslo, Report No. 36.
Sykes, J. B.: 1953, *Monthly Notices Roy. Astron. Soc.* **113**, 189.
Wanders, A. J. M.: 1934, *Z. Astrophys.* **8**, 108.
Wittmann, A.: 1973, *Solar Phys.* **29**, 333.
Zwann, C.: 1965, *Rech. Astron. Inst. Utrecht* **17,** (4).